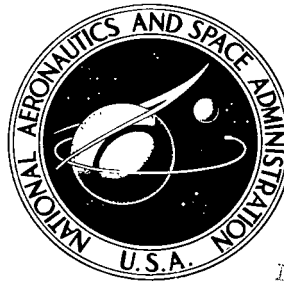


**NASA TECHNICAL NOTE**



**NASA TN D-5310**

c.1

NASA TN D-5310

ISSUED BY THE DIVISION OF  
TECHNICAL SERVICES  
WASHINGTON, D.C. 20546



TECH LIBRARY KAFB, NM

# **THERMOELASTIC INSTABILITY OF OPEN-SECTION BOOMS**

*by James H. Donohue and Harold P. Frisch*

*Goddard Space Flight Center  
Greenbelt, Md.*

NATIONAL AERONAUTICS AND SPACE ADMINISTRATION • WASHINGTON, D. C. • DECEMBER 1969



0132170

# THERMOELASTIC INSTABILITY OF OPEN-SECTION BOOMS

By James H. Donohue and Harold P. Frisch

Goddard Space Flight Center  
Greenbelt, Md.

NATIONAL AERONAUTICS AND SPACE ADMINISTRATION

---

For sale by the Clearinghouse for Federal Scientific and Technical Information  
Springfield, Virginia 22151 - Price \$3.00

## ABSTRACT

When the sun shines on a hollow cylindrical boom in space, a temperature gradient develops across the boom. The resulting differential thermal expansion generates a thermal bending-moment distribution along the boom, causing it to bend away from the sun. If the thermally bent boom is deflected in the out-of-plane direction (normal to sun-boom plane), twist is produced along the boom. Dynamic out-of-plane motion produces twist motion which, in conjunction with a thermal lag, causes the thermal bending moments to rotate. The component of the rotated thermal bending moment contributing toward out-of-plane motion is called the thermal drive. If it is of sufficient magnitude and properly phased, then the boom can be thermally pumped to produce a divergent oscillatory out-of-plane motion. Goddard Space Flight Center has developed two mathematical thermoelastic models of this phenomenon. Analysis substantiates the contention that the anomalous motion of the OGO-IV spacecraft was caused by an unstable, thermally induced oscillation of its open-section boom (standard STEM). The primary deficiency of an open-section is its weak torsional characteristic. The two- to three-orders-of-magnitude improvement in torsional rigidity (measured on several configurations having seams "zippered" by interlocking tabs) indicates that zippering the boom is the most practical way to avoid the thermally induced instability.

## CONTENTS

Abstract . . . . .	ii
INTRODUCTION . . . . .	1
INSTABILITY MECHANISM . . . . .	1
LUMPED-PARAMETER MODELS . . . . .	4
Linear Model . . . . .	4
Nonlinear Model . . . . .	7
DISTRIBUTED THERMOELASTIC VIBRATION MODEL . . . . .	9
TORSIONAL CHARACTERISTICS . . . . .	12
Laboratory Measurements . . . . .	12
Stability Ramifications of Torsional Nonlinearities . . . . .	13
CONCLUSIONS . . . . .	13
References . . . . .	14

# THERMOELASTIC INSTABILITY OF OPEN-SECTION BOOMS\*

by

James H. Donohue and Harold P. Frisch

*Goddard Space Flight Center*

## INTRODUCTION

Shortly after the deployment of the 60-foot open-section boom on OGO-IV, anomalous spacecraft motion was observed at the boom's natural frequency. Today, more than a year later, this oscillation still occurs except during solar eclipse. These facts have led to the hypothesis that the spacecraft is reacting to an unstable thermally induced oscillation of its boom. This document describes the results of both theoretical and experimental work done at GSFC which supports the contention that the anomalous spacecraft motion can be explained by the thermally induced oscillation theory.

## INSTABILITY MECHANISM

A simplified explanation of the instability mechanism is as follows. Consider an element of a thin-walled cylinder of unit length with its center axis normal to the sun line (Figure 1). Irradiation establishes around the cylinder a steady-state temperature distribution that is symmetric with respect to the X axis. Differential thermal expansion caused by the temperature gradient between the upper and lower halves of the cylinder produces a thermal bending-moment vector along the Y axis. The magnitude of this vector is proportional to the temperature gradient between the hot and cold spots.

A bending-moment vector can be defined in this manner at every element along the boom's length. The integrated effect of this bending-moment distribution causes the boom tip to deflect away from the sun. If the Z axis comes out of the paper, then this deflection is in the XZ plane and will be called "in-plane" deflection.

Now consider the cylindrical element to be spinning at constant speed about its center axis (Figure 2). The steady-state temperature distribution becomes fixed with respect to the inertial frame (Reference 1). The hot spot and cold spot rotate out of the XZ plane and are no longer diametrically opposed. Moreover, the temperature gradient (and hence, the magnitude of the thermal bending-moment vector) decreases between these points. The direction of the bending-moment vector is no longer along the Y axis, but is now inclined to it by what will be referred to

\*Presented at the Symposium on Gravity Gradient Attitude Control sponsored by the Air Force (SAMSO) and Aerospace Corporation, Los Angeles, Calif., Dec. 3-5, 1968.

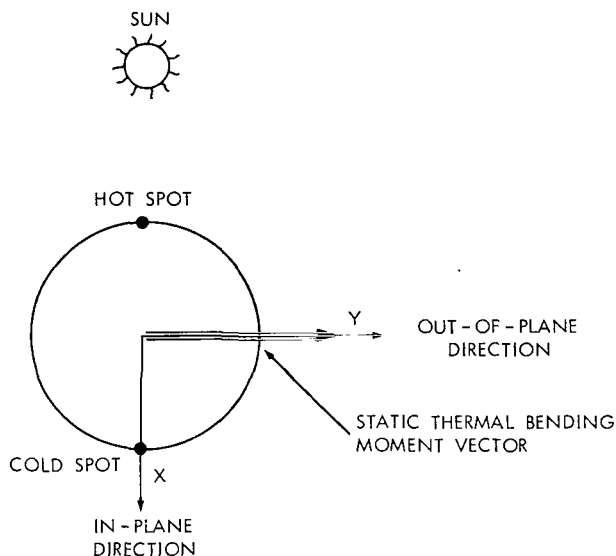


Figure 1—Cross-section of closed-section cylinder heated by solar radiation.

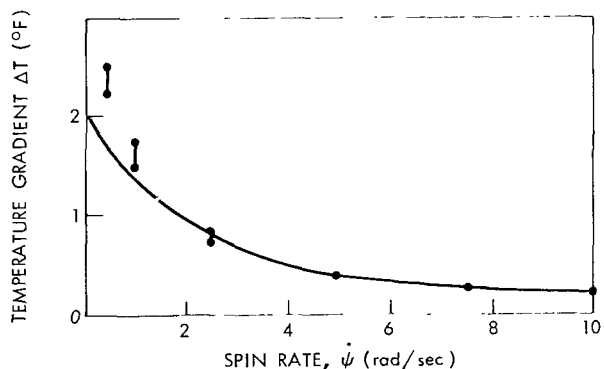
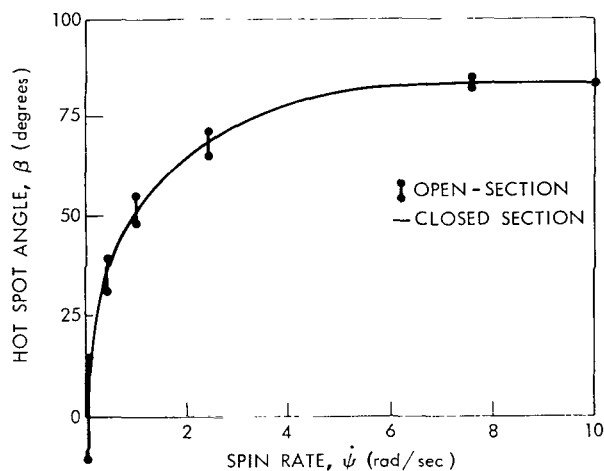


Figure 3—Thermal properties of thin-walled cylinders.

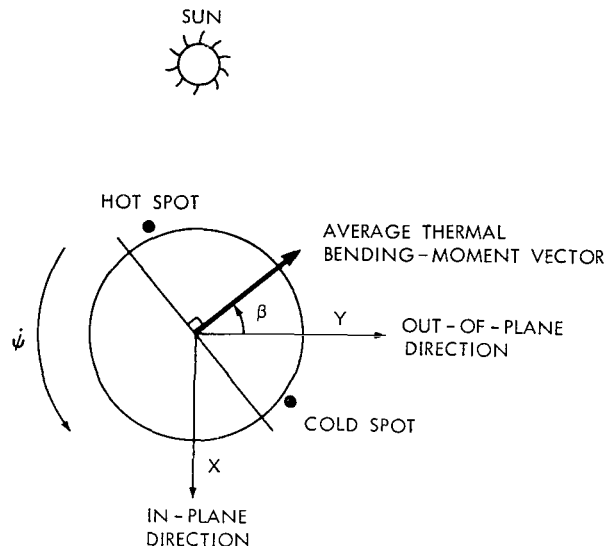


Figure 2—Steady-state, hot-spot position in sun coordinates for closed-section cylinder spinning at constant rate in solar thermal field.

as the "average hot-spot angle  $\beta$ ." The thermal bending-moment vector now has a component along the X axis which, when integrated as before, would deflect the tip in this out-of-plane direction.

Figure 3 shows the average hot-spot angle and temperature gradient with increase in spin rate for both closed- and open-section cylinders. As can be seen, good agreement exists between them. The variation in the open-section data results from the thermal discontinuities created by the seam of the open-section cylinder. Two very significant points are clear from these data: namely, as the spin rate increases, the hot-spot angle is limited, and the temperature gradient approaches zero.

The introduction of various linearizing assumptions will reveal the basic mechanism by which the boom is thermally excited. If the spin rate  $\dot{\psi}$  is small, then it is reasonable to assume that the thermal bending moment will be constant in magnitude and that its direction

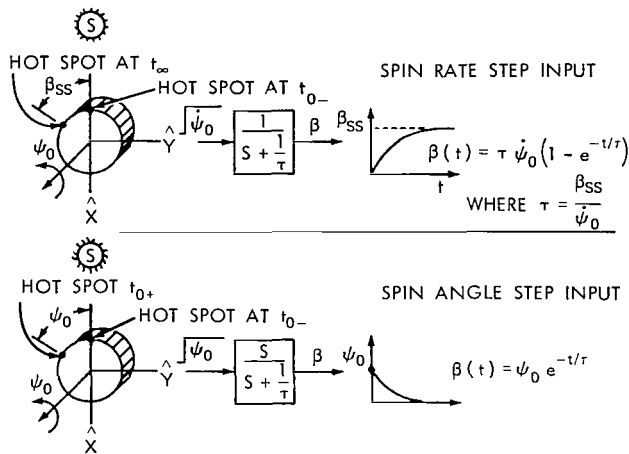


Figure 4—Hot-spot response.

will be defined by the hot-spot angle  $\beta$ . This angle is assumed to be adequately described by a simple lag with respect to the spin rate, an assumption consistent with predicted behavior for simple inputs (Figure 4).

For a step spin-rate input, the hot spot approaches the steady-state value exponentially; whereas, for an instantaneous rotation through the angle  $\psi_0$ , the hot-spot angle  $\beta$  decays exponentially from  $\psi_0$  to zero. The time lag for slow spin rates of the standard STEM (Storable Tubular Extendable Member) is approximately 2 seconds.

Consider a clamped, free beam normal to the sun and thermally bent in the in-plane direction (Figure 5). The magnitude of the in-plane tip deflection is termed  $\delta_T$ . A load applied at the tip of the thermally bent boom in the out-of-plane direction would deflect out of plane an amount  $\phi_T$  and twist an amount  $\psi_T$ . This twist comes about because the out-of-plane force applied at the tip of a thermally deflected boom produces a torque at all points along the boom's length. In the dynamic case, the out-of-plane acceleration of mass points along the boom produces the out-of-plane force. The resulting torque that induces torsional motion is referred to as whiplash torque.

For the model being developed, it is assumed that in-plane vibrational motion of the boom is of negligible amplitude and takes place about the boom's static, in-plane, thermally bent position (Figure 6). Any thermally induced vibrations will presumably occur in the out-of-plane direction.

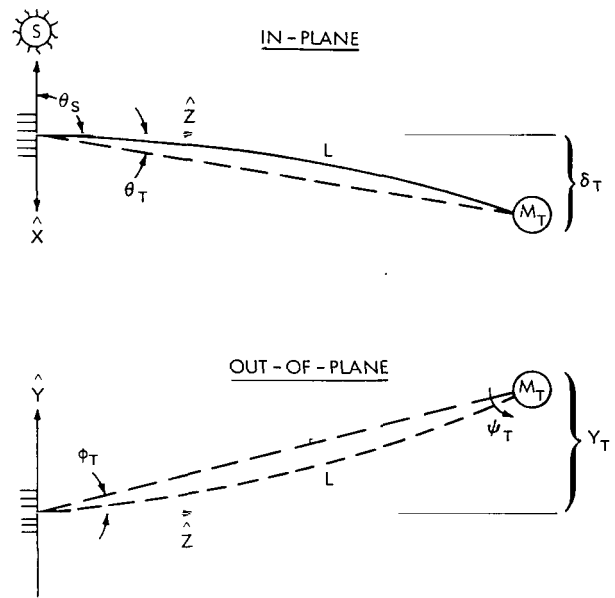


Figure 5—Boom geometry.

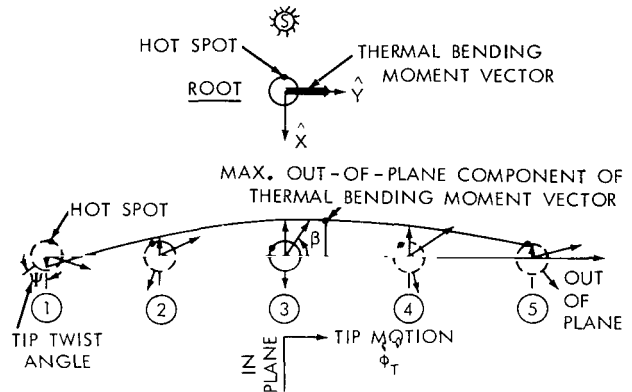


Figure 6—Generation of out-of-plane thermal bending-moment components through tip motion.

Associated with out-of-plane vibration is a certain amount of torsional motion that will affect the overall temperature distribution and, hence, the thermal bending-moment distribution. If the change in the thermal bending-moment distribution caused by hot-spot dynamics in the linear model is phased properly with twist and out-of-plane deflection, then thermal pumping can occur.

The static, thermal bending-moment distribution deflects the boom tip in the in-plane direction to position 3 of Figure 6. If the tip is deflected in the out-of-plane direction, the resulting twist distribution caused by whiplash torque causes hot-spot dynamics that generate thermal bending-moment components that tend to deflect the boom in the out-of-plane direction. As depicted in tip coordinates, the out-of-plane thermal bending-moment components during a half-cycle of an oscillation are out of phase with the tip twist angle because of the thermal lag of the hot spot. Assuming that twist angle is in phase with tip deflection, this nonsymmetric distribution of out-of-plane thermal bending-moment components causes the structural equilibrium point to shift during this half-cycle because of thermal deflection so that the deflection at point 5 is larger than the initial deflection at point 1. This phenomenon is reversed during the subsequent half-cycle; therefore, thermal pumping will always occur in the out-of-plane direction if structural damping is neglected.

## LUMPED-PARAMETER MODELS

### Linear Model

The signal-flow diagram of Figure 7 represents the linear lumped-parameter model of the boom motion. Structurally, the out-of-plane motion of the boom is modeled as a spring mass dashpot system in which tip motion in angular coordinates creates torques at the boom root that are proportional to displacement and displacement rate as indicated by the lower loop. The amount of twist at the boom tip, resulting from out-of-plane oscillation coupled through whiplash torque, is termed twist gain, denoted as  $K_3$  on the diagram. The hot-spot angle of the tip  $\phi_T$  is described by a simple lag with respect to the tip twist  $\psi_T$ . The thermal bending moment  $K_2$  is obtained from the static in-plane tip deflection  $\delta_T$  and the transverse spring constant  $K_1$ :

$$K_2 = K_1 \delta_T = \frac{3EI \delta_T}{L^2},$$

where

$E$  = Young's modulus of elasticity,

$I$  = geometrical moment-of-inertia about centroidal axis,

$\delta_T$  = static in-plane thermal deflection, and

$L$  = boom length.

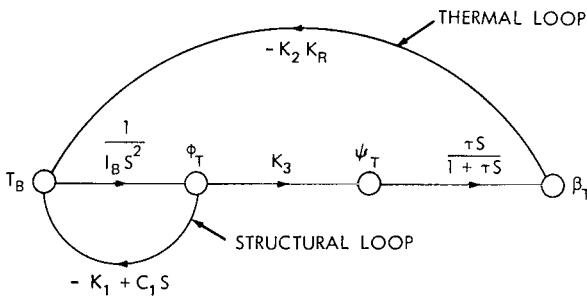


Figure 7—Signal-flow diagram of linear model.



The out-of-plane thermal bending moment is given by  $K_2 \sin \beta_T \approx K_2 \beta_T$ . Introduction of an additional constant  $K_R$  takes into account the integration of out-of-plane bending moment over the length of the boom (as required by the lumped-parameter approach). The importance of twist gain to the stability of this model is paramount since it directly influences the destabilizing thermal-feedback loop gain.

### Whiplash Torque

The inertial acceleration of the boom mass caused by sinusoidal out-of-plane motion creates inertial forces along the boom. If the boom is bent, then these forces produce whiplash torques along the boom. If the in-plane deflection curve is assumed to be invariant and the out-of-plane and in-plane deflection shapes are assumed to be parabolic, then the whiplash torque can be expressed as

$$T(Z, t) = -\omega^2 \rho_T \beta_T L^2 \sin \omega t \left[ \frac{L}{5} + \frac{M_T}{\rho} - Z \left( \frac{1}{2} + \frac{2M_T}{\rho L} \right) + Z^2 \left( \frac{1}{3L} + \frac{M_T}{\rho L^2} \right) + Z^3 \left( \frac{-1}{30L^4} \right) \right],$$

where

- $\omega = (12EI / \rho L^4)^{1/2}$  = out-of-plane vibration frequency,
- $\rho$  = mass density of boom per unit length,
- $M_T$  = tip mass,
- $\beta_T$  = out-of-plane tip deflection,
- $\alpha_T$  = in-plane tip deflection, and
- $L$  = boom length.

### Twist Gain

Variations in whiplash torque along the boom in conjunction with the torsional end constraints constitute a boundary value problem representing nonuniform twist as defined in Reference 2. Timoshenko's differential twist equation for open-section members is

$$\frac{d^3 \psi}{dZ^3} - \frac{C}{C_1} \frac{d\psi}{dZ} = - \frac{T(Z)}{C_1},$$

where

- $C$  = torsional rigidity,
- $C_1$  = warping rigidity, and
- $\psi$  = twist angle.

The torque is opposed by the warping rigidity and the torsional rigidity. The solution to this equation for short boom lengths ( $L < 30$  ft) is quite sensitive to the boundary conditions; that is, clamping both ends of the boom to prevent warping will increase the boom's effective torsional stiffness and reduce twist. Conversely, when both ends are pinned so that the ends are free to warp, the effective stiffness is decreased, and twist is increased.

If the torsional inertia is small, then the excitation frequency (out-of-plane vibration frequency) will be much less than the natural frequency in torsion. It is therefore reasonable to ignore the torsional dynamics and to assume that twist is proportional to the whiplash torque, which is in turn proportional to out-of-plane deflection. The ratio of twist to out-of-plane deflection as computed at the tip is called twist gain. Thus,

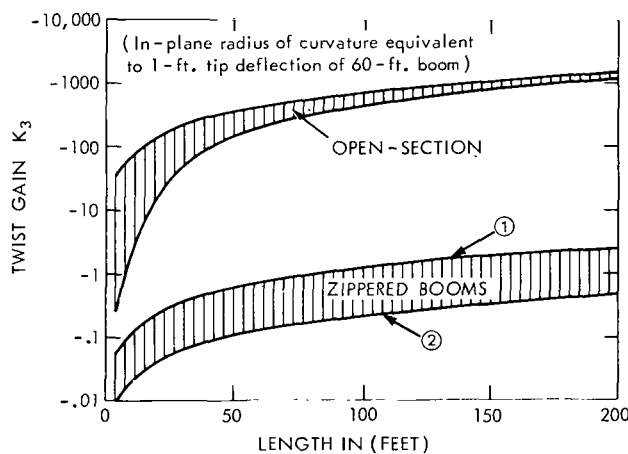


Figure 8—Twist gain (no tip mass).

$$K_3 = \frac{\psi_T}{\phi_T}$$

For zippered booms where warping is neglected, the twist gain is

$$K_3 = \frac{-\omega^2 \theta_T \rho L^4}{C} \left( \frac{1}{18} + \frac{M_T}{3\rho L} \right)$$

Figure 8 shows the twist gain as a function of length for the open section and two zippered-boom configurations (Table 1). Zippered booms are basically open-section members whose seams

are literally "zippered" by means of interlocking tabs, greatly increasing the torsional stiffness. Except at very short boom lengths (that is, below 30 feet), the twist gain of the open-section boom is two to three orders-of-magnitude larger than that of either of the zippered booms. Below the 30-ft mark, boundary conditions become very important in determining the twist gain of the open-section boom.

#### Minimum Required Damping Ratio

Figure 9 illustrates the minimum viscous damping ratio required to establish neutral stability as a function of length for the open-section and two zippered booms. To obtain comparative data for open and zippered booms of various lengths, the in-plane deflection of all booms is assumed to be along the same parabolic curve corresponding to a 1800-ft radius of curvature, equivalent to a 1-ft tip deflection of a 60-ft boom. The sun is assumed normal to the boom and a 2-second thermal time constant is used. The significance of the minimum required damping ratio is that if the tip of the boom were deflected slightly in the out-of-plane direction, it would oscillate without growing or decreasing in amplitude. For damping less than this value, the tip motion would diverge sinusoidally. The required damping for booms without tip mass increases up to 100 ft; beyond this

point, it settles out at 0.6 for the open-section and 0.0002 for the zippered boom. The basic reason for the three-orders-of-magnitude difference in the damping required is the decrease in twist gain resulting from the improvement in torsional rigidity,  $C$ , gained by zippering.

When  $\tau\omega \ll 1$ , the minimum required damping ratio can be expressed as

$$\zeta_{\min} = 1.6 \times 10^{-7} \left[ \frac{(\sin \theta_s)^2 \delta_{T_{60}}^2 (EI)^{3/2} K_R \tau}{C} \right] \times \left[ \frac{\rho L + 6M_T}{18 \rho^{3/2} L + 144 L^{-1/2} M_T^{3/2}} \right]$$

The effect of variation in other parameters is apparent from this expression. If the boom's wall is perforated, the temperature gradient across it will drop, causing a proportional decrease in tip deflection. Thus, the required damping will be reduced by the square of the change. Moreover, it varies proportionally with the square of the sine of the angle between the boom and sun line  $\theta_s$ , directly with the thermal time constant  $\tau$ , and inversely with the magnitude of the tip mass  $M_t$ . The 60-ft OGO-IV boom in this model requires a damping ratio of 0.2 for the clamped boundary condition.

## Nonlinear Model

After it has been determined on the basis of the linear model that the boom is unstable, the usefulness of this model ceases because it violates the small-angle assumptions. A determination of steady-state vibration amplitude must take into consideration the thermal nonlinearities that accompany high spin rates; an analog simulation performed at GSFC takes these into account. The effect of these thermal nonlinearities is to reduce the thermal feedback gain and to cause the amplitudes and rates to reach a steady-state solution. The amplitude of this oscillation is called flutter amplitude. Figure 10 shows this flutter amplitude for a 30-ft open-section boom whose static in-plane tip deflection is 0.5 foot and has a 0.01 viscous damping ratio.

The flutter amplitude is plotted against the reference twist gain ( $K_3 K_R$ ), which as noted earlier is highly dependent upon root boundary conditions for short booms. Note that the flutter amplitude

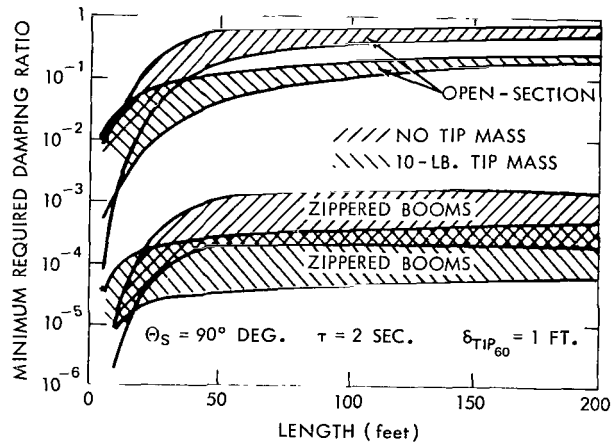


Figure 9—Minimum required damping ratio.

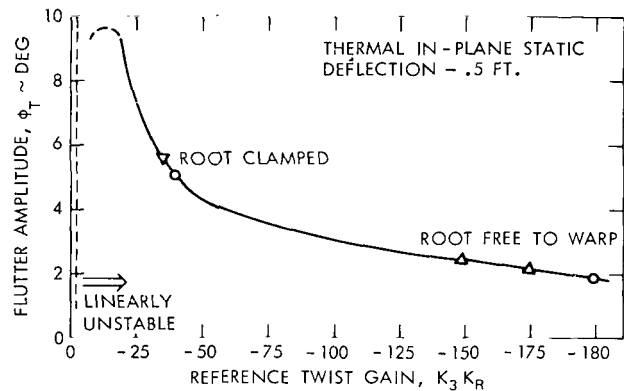


Figure 10—Pure analog results, steady-state flutter amplitude vs reference twist gain for 30-ft open-section (no tip mass,  $\zeta = 0.01$ ).

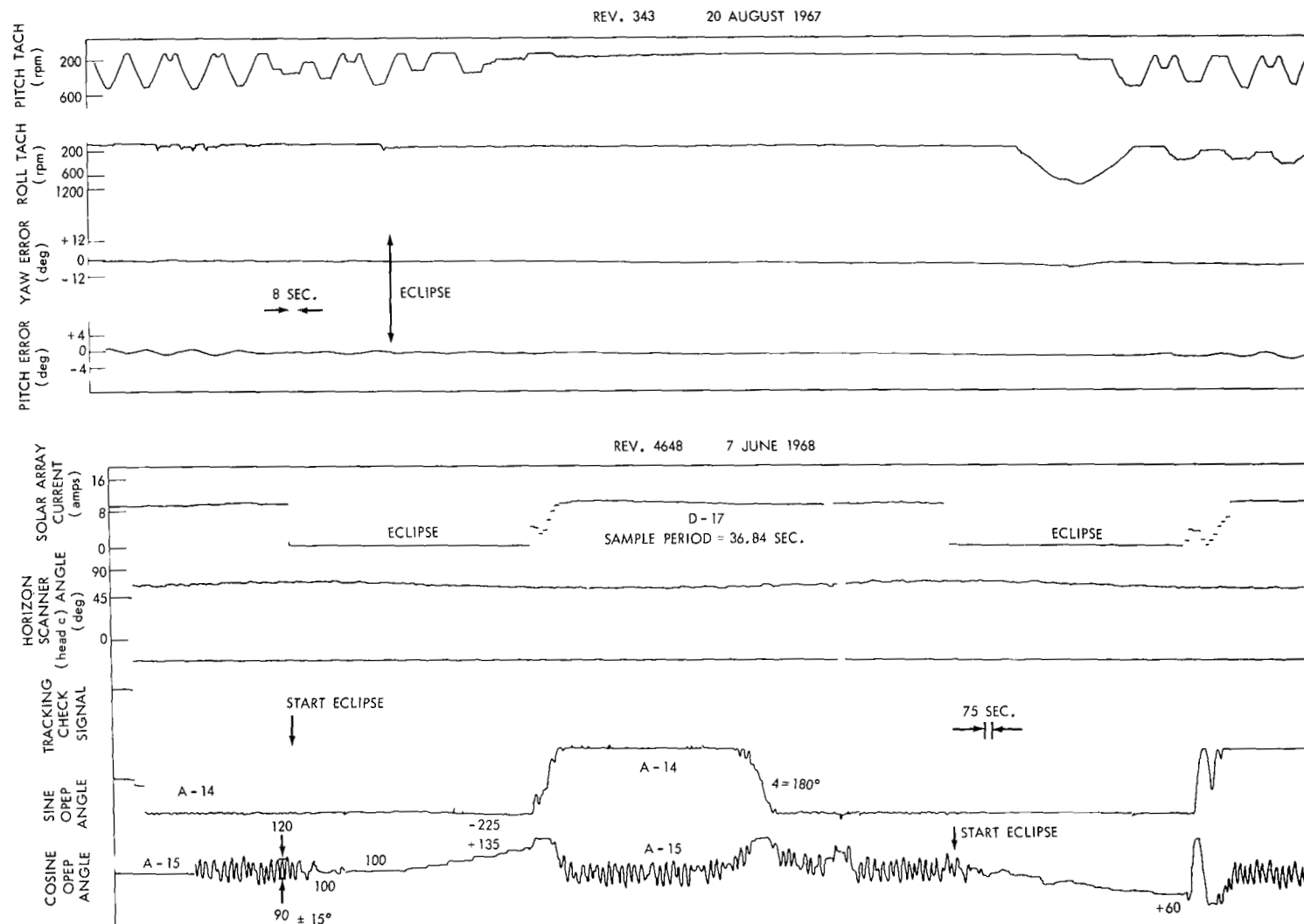


Figure 11—Thermal flutter data from OGO-IV.

is larger for the clamped-root condition than it is for the pinned-root condition; that is true because the effective torsional stiffness of a boom free to warp is less than that of a boom clamped at the root. Thus, for the same amount of out-of-plane oscillation, the torsionally weaker boom will twist more and enter more quickly into the stabilizing region of thermal nonlinearities.

### *Observed OGO Spacecraft Dynamics*

Figure 11 illustrates flutter data observed on OGO-IV, whose boom motion cannot be observed directly but must be inferred from spacecraft motion. The first set of data shows the spacecraft motion to be about 2 to 3 degrees peak-to-peak with a 40-second period, which is close to the first natural period of boom-satellite system. The oscillation is vividly observable from the momentum-wheel tachometer data, which show the motion subsiding within a few cycles after eclipse. This decay rate indicates the presence of an equivalent linear damping ratio of 0.05. The second set of data indicates spacecraft motion from data on the position of the orbit plane experiment package (OPEP). Normally, this package is positioned until its rate gyro senses no rate. However, boom flutter induces a spacecraft rate that results in dynamic positioning of the OPEP. This figure is interesting because it clearly reveals the continuous presence of boom flutter except during periods of eclipse, which are indicated by the solar-array current data. The boom-tip flutter half-amplitude associated with this motion is approximately 20 feet, which corresponds to 20 degrees in the angular notation.

### *OGO Simulation*

The OGO-IV spacecraft dynamics and control system were incorporated into the simulation of the thermal nonlinear model. Figure 12 shows results of a simulation of 20-degree boom-flutter half-amplitude, where the viscous damping ratio is 0.005. The spacecraft motion denoted by  $\theta$  in OGO notation oscillates approximately 3 degrees peak-to-peak. This magnitude of pitch motion exceeds the control-system dead bands, resulting in almost continuous operation of the momentum wheel and periodic activation of the gas jets. The thermal bending moment saturates at about 0.002 ft-lb, which would correspond to a static deflection of 2 inches. This saturation is caused by thermal nonlinearities that limit  $\beta$  to 60 degrees and attenuate the temperature gradient by 50 percent. The apparent discrepancy between the estimated 0.05 damping ratio observed after eclipse and the 0.005 used in this simulation probably arises from the viscous damping assumption and the fact that damping may differ significantly in and out of eclipse because of cross-sectional changes in the boom.

## **DISTRIBUTED THERMOELASTIC VIBRATION MODEL**

In addition to the lumped-parameter model, a more detailed analysis of the thermally induced vibration model has been simulated on a digital computer. The detailed equations are published in Reference 3. The boom is treated as a uniform, continuous thin-walled cylinder of open cross-section clamped at one end and free to deflect and warp at the other. This model assumes that the

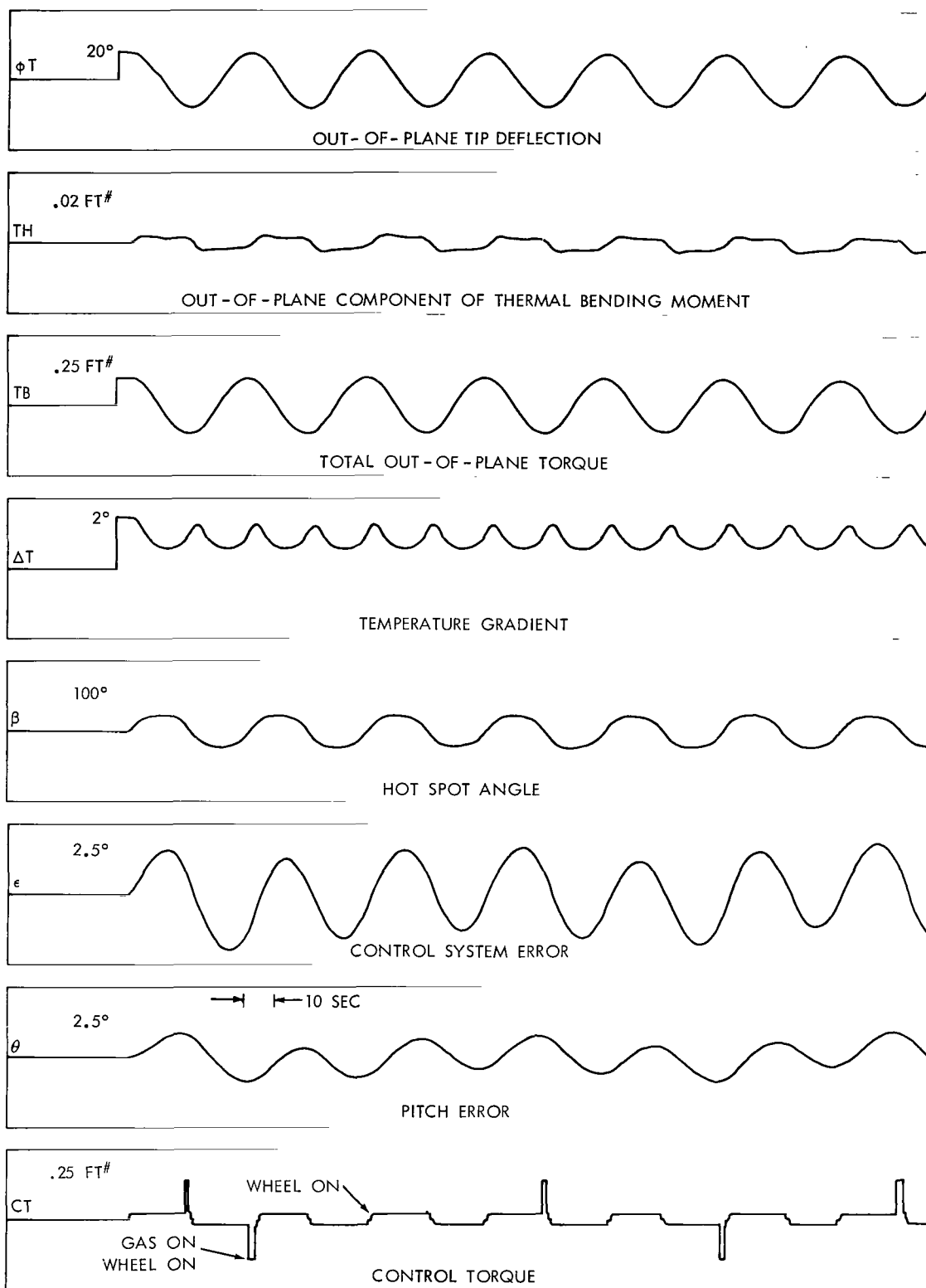


Figure 12—Pure analog thermal flutter simulation of OGO-IV; 60-ft boom,  $\zeta = 0.005$ ,  $K_3 K_R = 20$ .

transverse and torsional modes of vibration are structurally uncoupled from each other and that the actual transverse-torsional motion of the boom may be adequately defined by the dynamic response of its first three undamped, unforced, normal modes of vibration. That is, one mode defines in-plane motion, one defines out-of-plane motion, and one defines torsional motion.

The time history of the temperature distribution about any cross-section along the boom's length will depend upon its thermal time constants, the amplitude, and the frequency of its torsional oscillation. As the amplitude of torsional oscillations at the free end may be large in general, the only adequate method of determining the temperature distribution is to solve the thermodynamic equation of heat conduction and radiation. By assuming that heat is conducted only in the circumferential direction, it is possible to determine the time history of the entire temperature profile. This is done by solving the standard one-dimensional, partial differential equation of heat conduction and radiation at incrementally-spaced stations along the boom, simultaneously with the equations that define the boom's transverse-torsional motion. The results represent the use of as many as 60 stations along the boom's length to obtain the thermal profile.

The only forcing functions considered in the results to be shown are the thermal bending-moment distribution (readily obtainable from the continuous knowledge of the thermal profile) and the whiplash torque. This torque, which has been discussed, effectively defines the mechanism by which nonplanar transverse motion couples with, and drives, the boom in torsion.

The digital program developed to solve the derived equations has been used to study the effect on the standard STEM's response of changes in boom length, transverse damping ratio, and torsional rigidity.

Figure 13, a polar plot of the boom's tip as a function of time, shows the effect of a change in boom length for a standard STEM. The time coordinate is introduced by allowing the origin of the XY coordinate system to translate without rotating along the oblique axis at a constant rate. Although the 30-ft boom is unstable, its rate of amplitude buildup from zero initial conditions is much less than that of the 45- and 60-ft booms. For the time span shown here, the peak half-amplitudes are 19 ft, 13 ft, and 2 ft.

Figure 14 shows the effect of a change in the transverse damping ratio for a 60-foot standard STEM. The steady-state amplitude is strongly dependent upon this parameter and, if it could somehow be increased to about 0.1, the oscillations would be stable.

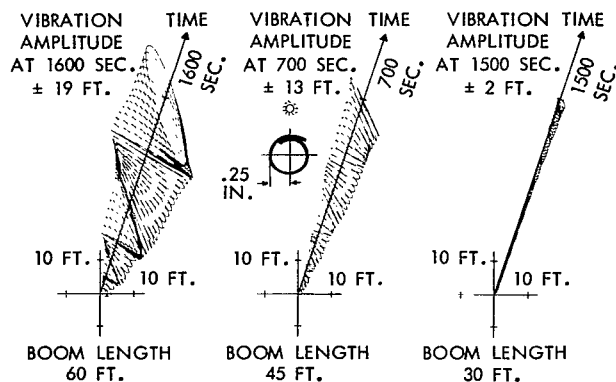


Figure 13—Effect of change in boom length on thermally induced vibrations for standard STEM (transverse damping ratio 0.005, torsional damping ratio 0.20, torsional rigidity 0.05 lb-in.<sup>2</sup>).

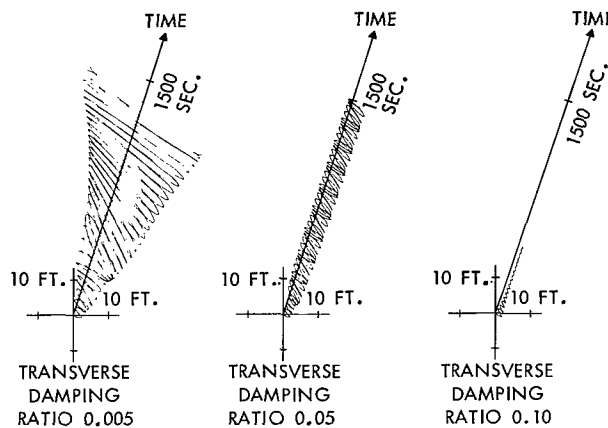


Figure 14—Effect of change in transverse damping ratio on thermally induced vibrations of standard STEM (boom length 60 ft, torsional damping ratio 0.10, torsional rigidity 0.05 lb-in.<sup>2</sup>).

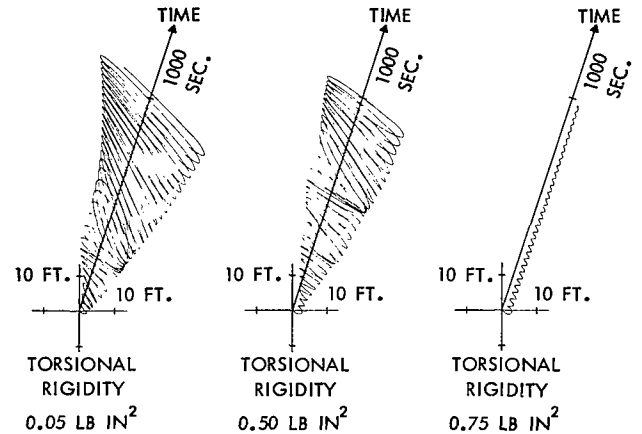


Figure 15—Effect of change in torsional rigidity on thermally induced vibrations of standard STEM (boom length 60 ft, transverse damping ratio 0.005, torsional damping ratio 0.10).

Figure 15 shows the effect of a change in the torsional rigidity of a 60-ft standard STEM. For booms having torsional rigidity equal to 0.05 lb-in<sup>2</sup> and 0.5 lb-in<sup>2</sup> (that is, standard STEM and ten times standard STEM), the response is not radically different; however, for torsional rigidity equal to 0.75 lb-in<sup>2</sup>, the thermal instability is eliminated. This result is in direct agreement with that shown previously on the flutter amplitude-versus-reference twist gain curve: that is, both analyses show a drop-off point, beyond which the thermal response rapidly improves.

Clearly, achieving stability requires either an unrealistically large amount of transverse damping or a realistically obtainable increase in the boom's torsional rigidity. Since a perforated boom with a zippered seam has a torsional rigidity equal to at least 40 times that shown on the 0.75 lb-in<sup>2</sup> curve and supposedly better thermal properties, it appears safe to assume that stability can be obtained.

## TORSIONAL CHARACTERISTICS

### Laboratory Measurements

For the past several months, torsional tests on several zippered-boom configurations have been performed at GSFC. Different manufacturers have used various means of zippering the boom's seam, all involving the meshing along a seam of teeth or tabs that restrict the boom's ability to warp. If the tabs are slightly undersized, a certain amount of twisting can occur before the teeth lock up; if the tabs are prestressed to lie firmly on the boom surface, a certain amount of torque is needed to break the frictional bond. Table 1 shows measured values for breakaway torque  $T_0$ , the angular rotation required to cause the teeth to lock up  $\psi_0$ , and the torsional rigidity after lockup  $c$ . These data reflect a boom of 30-ft length. The weakest zippered configuration is two orders-of-magnitude stiffer than the open-section boom. For the zippered booms, the damping requirement is reduced to a negligible level.



The variation in torsional rigidity is primarily a function of the number of interlock tabs per unit length. The high torsional rigidity of the double-zipper configuration is not caused by the two interlock seams but rather by the small tab spacing along a seam.

## Stability Ramifications of Torsional Nonlinearities

Figure 16 is a block diagram of the linear lumped-parameter model; the torsional nonlinearities of zippered booms are incorporated in the thermal loop and represented as  $G_N$ . The vertical height of this hysteresis loop represents the total twist dead space before teeth lockup, whereas the horizontal break point represents the magnitude of the frictional breakaway torque. The slope in the horizontal direction is proportionate to the inverse of the torsional rigidity. A describing function analysis of this system showed that twist dead space should be minimized in order to prevent the possibility of boom-limit cycle of a normally stable system, should the frictional bond be broken.

Keeping the frictional bond intact prevents warping along the boom's span, and it basically

acts as a closed-section cylinder  $3 \cdot 10^4$  times stiffer torsionally than an open section. This conclusion is also true when the frictional bond in the overlap of the open-section boom is not broken, which could explain why thermal oscillations did not proceed continuously on OGO-V. Another boom configuration presently being evaluated at GSFC consists of two open-section elements, one inserted inside the other in opposed direction with respect to the seam. Neglecting frictional effects, this boom is no stiffer torsionally than the single element; however, by using surfaces of high frictional characteristics and by making the naturally formed radius of the inner element greater than that of the outside element, it may be possible to increase the breakaway torque beyond the normally expected value from external sources. This boom could be considered a closed section; however, extensive tests would be required to evaluate the long-term variations in its frictional characteristics.

## CONCLUSIONS

The abnormal behavior of the OGO-IV spacecraft in sunlight is explainable by the thermally induced boom-oscillation theory. Results of the simple lumped-parameter model and the complex

Table 1

Configuration	Torsional rigidity, C (lb in. <sup>2</sup> )	Twist dead space, $\psi_0$ (deg)	Breakaway torque, $T_0$ (oz)
Open section (unperforated)	0.058	—	—
Zippered (perforated) ①	30	$\pm 10$	0.18
Zippered (perforated) ②	85	$\pm 450$	0.18
Double zipper (perforated)	213	$\pm 4.5$	1.2

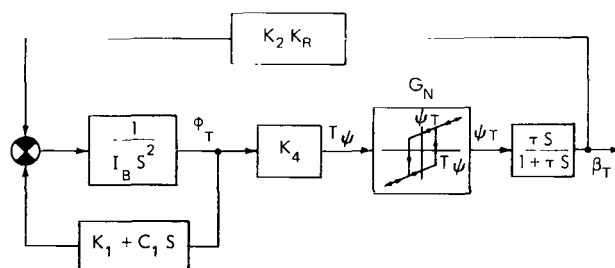


Figure 16—Block diagram, linear model with torsional nonlinearity (zippered boom).

distributed thermoelastic model show that thermal oscillations can be prevented (or at least that flutter amplitude can be reduced) by perforating the boom, decreasing the absorptivity, increasing the thermal lag, or increasing bending damping. However, all these approaches are of questionable value; the most reasonable approach is to significantly stiffen the boom in torsion. Moreover, the concept of tightly zippering the boom is the most practical solution because it gains two to three orders-of-magnitude over the standard STEM in torsional stiffness, serving to reduce the required damping to realistic values.

Goddard Space Flight Center  
National Aeronautics and Space Administration  
Greenbelt, Maryland, March 24, 1969  
160-76-01-01-51

## REFERENCES

1. Charnes, A., and Raynor, S., "Solar Heating of Rotating Cylindrical Space Vehicle," *ARS Journal*, 30(5): 479-484, May 1960.
2. Timoshenko, S., "Theory of Bending, Torsion, and Buckling of Thin-Walled Members of Open Cross Section," *Journal of the Franklin Institute*, 239(4), 1945.
3. Frisch, H. P., "Thermally Induced Vibrations of Long Thin-Walled Cylinder of Open Section," ASME/AIAA, 10th Annual Structures, Structural Dynamics, and Materials Conference, New Orleans, La., April 14 to 16, 1969.

NATIONAL AERONAUTICS AND SPACE ADMINISTRATION  
WASHINGTON, D. C. 20546  
OFFICIAL BUSINESS

FIRST CLASS MAIL



POSTAGE AND FEES PAID  
NATIONAL AERONAUTICS AND  
SPACE ADMINISTRATION

010 071 57 51 385 69321 00003  
AIR FORCE WEAPONS LABORATORY/ALTL/  
KIRTLAND AIR FORCE BASE, NEW MEXICO 8111

REF ID: A64521, 0107157, 69321, 00003

POSTMASTER: If Undeliverable (Section 158  
Postal Manual) Do Not Return

*"The aeronautical and space activities of the United States shall be conducted so as to contribute . . . to the expansion of human knowledge of phenomena in the atmosphere and space. The Administration shall provide for the widest practicable and appropriate dissemination of information concerning its activities and the results thereof."*

— NATIONAL AERONAUTICS AND SPACE ACT OF 1958

## NASA SCIENTIFIC AND TECHNICAL PUBLICATIONS

**TECHNICAL REPORTS:** Scientific and technical information considered important, complete, and a lasting contribution to existing knowledge.

**TECHNICAL NOTES:** Information less broad in scope but nevertheless of importance as a contribution to existing knowledge.

**TECHNICAL MEMORANDUMS:** Information receiving limited distribution because of preliminary data, security classification, or other reasons.

**CONTRACTOR REPORTS:** Scientific and technical information generated under a NASA contract or grant and considered an important contribution to existing knowledge.

**TECHNICAL TRANSLATIONS:** Information published in a foreign language considered to merit NASA distribution in English.

**SPECIAL PUBLICATIONS:** Information derived from or of value to NASA activities. Publications include conference proceedings, monographs, data compilations, handbooks, sourcebooks, and special bibliographies.

**TECHNOLOGY UTILIZATION PUBLICATIONS:** Information on technology used by NASA that may be of particular interest in commercial and other non-aerospace applications. Publications include Tech Briefs, Technology Utilization Reports and Notes, and Technology Surveys.

*Details on the availability of these publications may be obtained from:*

SCIENTIFIC AND TECHNICAL INFORMATION DIVISION  
NATIONAL AERONAUTICS AND SPACE ADMINISTRATION  
Washington, D.C. 20546